Mapping the Active Site−Ligand Interactions of Orotidine 5′-Monophosphate Decarboxylase by Crystallography[†,‡]

Ning Wu,[§,||] Wanda Gillon,[§,||] and Emil F. Pai*[,§,||,⊥,#]

Departments of Biochemistry, Molecular & Medical Genetics, and Medical Biophysics, and Protein Engineering Network, Centres of Excellence, University of Toronto, 1 King's College Circle, Toronto, Ontario M5S 1A8, Canada, and Division of Molecular and Structural Biology, Ontario Cancer Institute, University Health Network, 610 University Avenue, Toronto, Ontario M5G 2M9, Canada

Received September 10, 2001; Revised Manuscript Received January 4, 2002

ABSTRACT: The crystal structures of orotidine 5′-monophosphate decarboxylases from four different sources have been published recently. However, the detailed mechanism of catalysis of the most proficient enzyme known to date remains elusive. As the ligand−protein interactions at the orotate binding site are crucial to the understanding of this enzyme, we mutated several of the residues surrounding the aromatic part of the substrate, individually and in combination. The ensuing effects on enzyme structure and stability were characterized by X-ray crystallography of inhibitor, product, or substrate complexes and by chemical denaturation with guanidine hydrochloride, respectively. The results are consistent with the residues $K^{42}D^{70}K^{72}D^{75B}$ being charged and forming an 'alternate charge network' around the reactive part of the substrate. In addition to exerting charge−charge repulsion on the orotate carboxylate, Asp^{70} also makes a crucial contribution to enzyme stability. Consequently, orotidine 5′-monophosphate decarboxylases seem to require the presence of a negative charge at this position for catalysis as well as for correct and stable folding.

Orotidine 5′-monophosphate decarboxylase (ODCase) catalyzes the last step of *de novo* pyrimidine synthesis (Scheme 1) (*1*). Most decarboxylases use either pyridoxal 5′-phosphate, metal ions, or delocalization into aromatic systems to stabilize the charge developing in the transition state for reaction acceleration (*2*). ODCase, however, does not employ any cofactors or metal ions (*3*, *4*), and the orotidine base of its substrate OMP is unable to delocalize the charge of the carbanion created upon the release of CO_2. Nevertheless, the enzyme accelerates the decarboxylation reaction by 17 orders of magnitude over the corresponding reaction in water of neutral pH, making ODCase the most proficient protein catalyst known. This remarkable property has caused the enzyme's mechanism to become the subject of major scientific interest (*5*−*9*).

Scheme 1

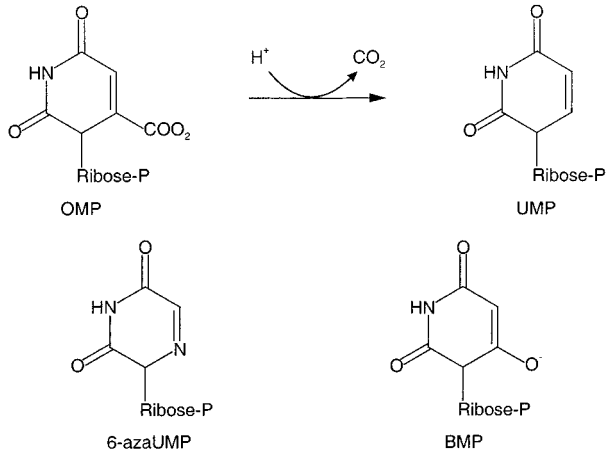

Recently, the structures of ODCases isolated from four different microorganisms and complexed to various ligands have been determined by X-ray crystallography (*10*−*13*). The results of those experiments have ruled out some of the previously proposed mechanisms but were still not sufficient to settle all open mechanistic questions (*14*−*17*).

Based on our own crystallographic and computational results (*10*), we have supported the idea that ODCase provides an example of what Jencks called the "Circe effect" (*18*). In this model of enzymatic catalysis, the binding energy supplied by one part of the substrate (phosphate and ribose in the case of ODCase) is utilized to elevate the energy level of the reactive part of the substrate (the orotidine base for ODCase). Described in brief for *Methanobacterium thermoautotrophicum* ODCase (*10*), the ribose phosphate moiety

[†] Use of the Advanced Photon Source was supported by the Basic Energy Sciences, Office of Science, U.S. Depatment of Energy, under Contract W-31-109-Eng-38. Use of the BioCARS Sector 14 was supported by the National Center for Research Resources, National Institutes of Health, under Grant RR07707.

[‡] The atomic coordinates for the various complexes have been deposited in the Protein DataBank, Research Collaboratory for Structural Bioinformatics, Rutgers University, New Brunswick, NJ (http://www.rcsb.org) under the codes 1KLY, 1KLZ, 1KM0, 1KM1, 1KM2, 1KM3, 1KM4, 1KM5, 1KM6.

* To whom correspondence should be addressed. Email: pai@hera.med.utoronto.ca.

[§] Department of Biochemistry, University of Toronto.

[||] Division of Molecular and Structural Biology, Ontario Cancer Institute.

[⊥] Departments of Molecular & Medical Genetics and of Medical Biophysics, University of Toronto.

[#] Protein Engineering Network, Centres of Excellence, University of Toronto.

10.1021/bi015758p CCC: $22.00
Published on Web 02/27/2002

is very tightly held by four hydrogen bonds (two bonds to each of the ribose hydroxyls), an ionic interaction between the side chain of a conserved arginine residue and the 5′-phosphate, and through hydrogen bonds from backbone atoms to the same phosphate, either directly or indirectly via water molecules belonging to the phophate's first hydration shell.

We postulated that most of this binding energy is used by the enzyme to force the orotate group into a partly hydrophobic cavity that is too small to accept the orotidine ring, and especially the carboxylate group, without steric clashes. This cavity also contains a system of alternating acidic and basic residues, K^{42}, D^{70}, K^{72}, and D^{75B}, aligned alongside the edge of the orotidine base. The side chain of D^{70} will create strong charge repulsion and even spatial overlap with the substrate's carboxylate group when the intact substrate base is modeled into the active site according to the binding position found for the competitive inhibitor 6-azauracil in *M. thermoautotrophicum* ODCase (*10*). In addition, completely desolvating a charged group and transferring it into a more hydrophobic environment are energetically very costly. Under such circumstances, orotate will be much more prone to shed its carboxylate group, thereby not only releasing spatial strain but also transferring the negative charge, which resided on the protruding carboxylate, away from D^{70} onto C6 of the orotidine ring. K^{72}, with its ammonium group already at hydrogen bond distance from the resulting carbanion, is in perfect position to supply the proton necessary for neutralization. As its side chain's amino group is now uncharged, it can no longer counter the charge−charge repulsion between the closely spaced aspartates D^{70} and D^{75B}. This, in turn, could lead to destabilization of the dimer, potentially opening up the active site and leading to product release.

Kinetic studies by Miller et al. have established the great importance of the contribution to binding energy provided by the ribose phosphate group (*19*). In the yeast enzyme, mutating the phosphate binding residues (Y127A/R235A) reduces k_{cat}/K_m by more than 10^7-fold, a finding that is reinforced by the fact that the enzyme does not decarboxylate orotic acid. For this substrate, k_{cat}/K_m is lowered by more than 12 orders of magnitude.

In an effort to better determine the function of each residue that surrounds the substrate's pyrimidine base and thereby shed more light on this elusive but remarkably efficient catalytic mechanism, we have determined the crystal structures of several active site mutants of *M. thermoautotrophicum* ODCase complexed with a variety of ligands, including substrate, product, and inhibitors. We have also probed the stability of some of the mutant proteins toward guanidine hydrochloride denaturation.

EXPERIMENTAL PROCEDURES

Cloning, Protein Expression, and Purification. The *M. thermoautotrophicum* ODCase gene was cloned as previously described (*20*). Site-directed mutagenesis was carrried out with the QuickChange kit from Stratagene. For each mutation, a complementary pair of primers was designed. The coding strand sequences are shown below with the mutation inducing codons in boldface type and underlined:

K42A: GGGAATACATAGACACGGTC**GCG**ATAGGGTACCCCC

D70G: GCAGAATCATAGCC**GGC**TTCAAGGTTGCAGATATACCCG

D70A: GCAGAATCATAGCC**GCC**TTCAAGGTTGCAGATATACCCG

D70N: GCAGAATCATAGCC**AAC**TTCAAGGTTGCAGATATACCCG

K72A: GCAGAATCATAGCCGACTTC**GCG**GTTGCAGATATACCCG

D70AK72A: GCAGAATCATAGCC**GCGTTCGCG**GTTGCAGATATACCCGAGACC

$D75^B$N: GCCGACTTCAAGGTTGCA**AAC**ATACCCGAGACCAATG

S127A: CCTCCTGACAGAGATG**GCA**CACCCAGGGGCAGAG

Q185A: GGTGTGGGAGCC**GCG**GGAGGCGACCCAGGGGAGACCC

The coding sequences for the D70A and K72A mutants were cut out of the standard pET15b vector at the *Nco*I and *Bam*HI sites and religated into the pProEXHTc vector (Lifetechnologies, Gibco BRL) for expression in SKP10 cells that did not contain the T7 polymerase gene. SKP10 cells are derived from the XL1 Blue cell line and carry a nonfunctional endogenous ODCase gene preventing background activity due to contamination with bacterial enzyme (*21*). Thrombin was used to remove the N-terminal His_6-tags as previously (*20*). All other mutant proteins were expressed and purified following procedures recently published for native enzyme (*20*).

For stability studies, site-directed mutagenesis was used again to create proteins truncated after residue 222. This ensures that a C-terminal helix attached to the native protein by a read-through artifact does not introduce spurious results. In addition to removing the pET15b vector-encoded amino acids, the six C-terminal residues of native ODCase are cutoff as well. These last six residues, however, are not visible in any of our crystal structures, and therefore are very flexible and presumably without significant influence on the protein's stability.

Crystallization, Data Collection, and Processing. For crystallization trials, all proteins were transferred into solutions of 20 mM HEPES, pH 7.5, 150 mM NaCl, and 3 mM DTT. Originally, crystals of all mutant proteins appeared in conditions very similar to the ones described for native *M. thermoautotrophicum* ODCase complexed with 6-azaUMP (1.2 M trisodium citrate, pH 6.5−8.5). However, most of the crystals were highly twinned and not suitable for diffraction studies. To obtain single crystals, 3−5% dioxane had to be added to the crystallization solution. The resulting crystals belonged to the higher symmetry space group $C222_1$.

All crystals were mounted in cryoloops and flash-frozen in a stream of boiling nitrogen using 12% (v/v) ethylene glycol as cryoprotectant. Diffraction data at a wavelength of 1.00 Å were collected at 100 K at beamlines BM14C and BM14D, BioCARS, APS, using Q4 area detectors (ACSD). Data were reduced using DENZO and scaled using SCALEPACK (*22*). Data collection statistics are given in Table 1. Most mutant proteins crystallized in space group $C222_1$; their unit cell axes varied by less than 1% from a = 58 Å, b = 103 Å, c = 74 Å. The D70N mutant crystallized in space group *P1* with unit cell parameters a = 59.8 Å, b = 59.9 Å, c = 73.9 Å, α = 97.3°, β = 100.1°, γ = 106.9°, and the S127A mutant crystals belonged to space group $P2_1$ with a = 58.3 Å, b = 73.8 Å, c = 59.4 Å, β = 119.4°.

Structure Determination. Applying various molecular replacement software packages, the monomer of the wild-

Table 1: Data Collection and Refinement Statistics

	K42A	D70G	D70A	D70N	K72A	D70AK72A	D75^{B}N	S127A	Q185A
Diffraction Data									
resolution (Å)	1.5	1.5	1.5	1.7	1.5	1.5	1.5	1.6	1.5
measured reflections (*n*)	486020	561988	306500	452529	506092	403208	294980	530511	402681
unique reflections (*n*)	33670	35507	35260	96504	35285	34794	34281	55090	34229
completeness (%)	93.7	98.0	97.2	92.5	98.3	96.4	95.0	95.1	95.3
R_{sym} (%)	4.4	4.9	4.9	3.8	4.3	4.2	3.6	5.1	5.4
space group	$C222_1$	$C222_1$	$C222_1$	*P1*	$C222_1$	$C222_1$	$C222_1$	$P2_1$	$C222_1$
molecule in A.U. (*n*)	1	1	1	4	1	1	1	2	1
Refinement Statistics									
resolution (Å)	30−1.5	30−1.5	30−1.5	30−1.7	30−1.5	30−1.5	30−1.5	30−1.6	30−1.5
protein atoms (*n*)	1631	1655	1628	6822	1640	1652	1626	3258	1648
water molecules (*n*)	225	219	210	487	271	207	221	321	210
reflections used for R_{free} (*n*)	2548	2616	2833	3378	2649	2613	2573	1666	2546
R_{cryst} (%)	16.2	16.7	17.7	17.9	15.5	17.0	16.5	17.7	16.9
R_{free} (%)	19.2	19.1	19.9	21.0	18.3	19.4	19.5	19.1	19.8
rmsd bond length (Å)	0.010	0.011	0.011	0.010	0.011	0.011	0.010	0.009	0.012
rmsd bond angle (deg)	1.5	1.5	1.5	1.5	1.6	1.5	1.5	1.5	1.6
average *B*-factor (Å^2)	14.6	14.3	14.6	21.0	12.3	16.8	15.3	17.9	17.0

Table 2: Active Site Compound

	K42A	D70G	D70A	D70N	K72A	D70AK72A	D75^{B}N	S127A	Q185A
intended	azaUMP	azaUMP	OMP	azaUMP	OMP	OMP	azaUMP	azaUMP	azaUMP
observed	azaUMP + H_2O	50% base flip	UMP + Cl^-	100% base flip	UMP	OMP	azaUMP + Cl^-	50% base flip	azaUMP + H_2O

type free enzyme was used as a search model. In cases where there were only one or two molecules per asymmetric unit, the program package CNS, version 0.9 (*23*), was used to find the cross-rotation and translation solutions. For D70N, for which we expected four molecules per asymmetric unit, the program EPMR (*24*) was applied. It found the first three molecules using the default settings. The fourth one was determined by mapping a dimer onto the monomer that did not have a partner, using the lsq command in the program package O (*25*). The subsequent refinement protocol, including rigid-body, simulated annealing, individual *B*-factors, least-squares minimization, and water picking, was carried out with the program CNS. Given the high observables-to-parameters ratio, no noncrystallographic symmetry restraints were used in the final refinement of D70N and S127A. Refinement statistics are included in Table 1.

For the alternate conformation of 6-azaUMP in the active sites of D70G and S127A structures, the occupancy of each conformation was set to 50% based on inspection of electron density maps (very similar density cutoffs), and *B*-factor refinement was used to absorb any deviation thereof. The chloride ions in the D70A and D75^{B}N structures were first assigned due to their interactions with positively charged side chains and their corresponding high electron density ($>8.5\sigma$) which made water molecules very unprobable candidates. This assignment was followed by a *B*-factor refinement, resulting in values for the Cl^- ions very similar to those of surrounding protein atoms. For the lysine mutants K42A and K72A, we were not able to conclusively decide whether the active site had incorporated a Na^+ ion, analogous to the Cl^- in the D70A mutant, or a water molecule because Na^+ and water have the same number of electrons and similar ligand shell geometries. We settled on assigning water molecules because the shape of the corresponding density was not as perfectly round as would be expected for a sodium cation.

Guanidine Hydrochloride Denaturation Studies. Guanidine hydrochloride (GnHCl) titrations were done at monomeric protein concentrations ranging from 8 to 32 μM in 20 mM Tris, pH 7.5, buffer with 50 mM NaCl and 0.5 mM TCEP [tris(2-carboxyethyl)phosphine hydrochloride]. The aliquots containing varying concentrations of GnHCl were allowed to equilibrate overnight before recording the ellipticity values at 25 °C. CD measurements were performed in an Aviv 62A DS circular dichroism spectrometer, monitoring the change in ellipticity at 222 nm in a 0.1 cm cuvette. The denaturation data were fit by nonlinear least-squares regression assuming a two-state transition using the program Prism (*26*).

RESULTS AND DISCUSSION

Inspection of the high-resolution electron density maps of the various complexes readily revealed that not all ligands bound to the mutant active sites were the same as the ones added to the crystallization setups (Table 2). While 6-azaUMP, due to its unreactive nature, did not change, the substrate OMP was always converted to the product UMP except when complexed to the double mutant D70A/K72A, although previous kinetic studies had characterized mutants D70A or K72A as catalytically inactive (*16*).

Although the ODCase complexes that were the subjects of this study adopted three different space groups (Table 1), major structural rearrangements were restricted to the relative orientation of dimers (rmsd for the positions of 417 C_α atoms in a dimer is 0.4 Å overall and 0.2 Å for 45 backbone and C_β atoms of conserved active site residues) (Figure 1).

Orotate Recognition Mutants: S127A and Q185A. For discussion purposes, the ring of orotidic acid can be divided into two halves: one that resembles the molecular structure of urea and a second one that carries the carboxylate group. The former half is used by ODCase to select for the proper base in its substrate OMP by providing an intricate hydrogen bonding network assembled from residues Ser^{127} and Gln^{185} and designed to sense the presence of the appropriate donors or acceptors at positions 2, 3, and 4 of the aromatic ring. In

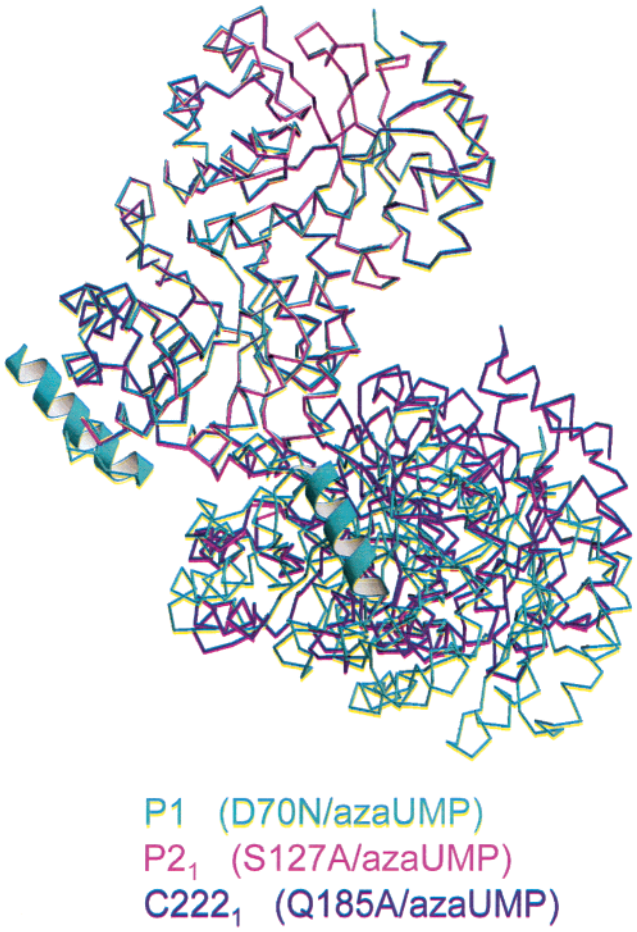

FIGURE 1: Crystal packing of the three different crystal forms of the mutant complexes. All four monomers in the unit cell of the *P1* space group (D70N/6-azaUMP) are shown. The backbones of the dimers do not show any significant deviation, as shown in the overlay of the dimer on top. The difference in packing is due to the rotation of dimers relative to each other. The ribbon helix indicates the ordered extra helix from the pET15b vector due to packing in the *P1* space group (*10*).

all the structures of *M. thermoautotrophicum* ODCase determined so far, native/6-azaUMP complex (*10*) as well as mutants described here, the main chain nitrogen of Ser^{127} interacts with the O4 atom of the ring whereas its side chain hydroxyl group serves as an acceptor to N3. The side chain of Gln^{185} adopts alternate positions with a water molecule shared between the phosphate and O2 in the native structure while its amide group binds directly to O2 and the Ser^{127} side chain in all the mutant structures.

The analysis of the S127A/6-azaUMP complex reveals a seemingly equal probability for the azauracil ring to adopt one of two orientations, distinguished from each other through a 180° rotation around the N1−C4′ bond (Figure 2A). The H-bond between the Ser^{127} side chain and N3 contributes to the correct placement of the orotate ring in the active site, and its loss allows the ring also to assume the lower energy *anti*-conformation found in solution (*27*). Given the approximately equal occupancy of both ring orientations in this mutant, one has to conclude that the Gln^{185} to O2 and Lys^{72} to N6 bonds are stronger than those formed when the interacting partners are switched and thereby compensate for the energetically less favorable syn-conformation of the nucleotide.

When O2 is located on top of the ribose ring, as found in the native enzyme−inhibitor/product structures (*10*−*13*), the 5′-phosphate and O2 can share a common proton donor. In ODCase, this role is played by the side chain of Gln^{185}, a residue highly conserved during evolution (*28*). It is the central residue in the loop comprising amino acids 180−190, a structural feature that is mobile in the free enzyme but closes down on the bound substrate, assuming a well-defined conformation. If this amino acid is mutated to alanine, the void created by the missing side chain atoms is filled with a chain of well-ordered water molecules (Figure 2B). One of these waters occupies the position of the Gln^{185} side chain amide nitrogen and undergoes hydrogen bonding to both the 5′-phosphate and O2. Therefore, structurally as well as energetically, this residue does not seem to be as essential as Ser^{127} in the enzyme's interaction with OMP. This interpretation is confirmed by Miller et al., who showed that this residue is dispensable in catalysis (*16*).

Probing the Acidic Residues of the Active Site's Alternating Charge Chain. If electrostatic repulsion is a major factor in ODCase catalysis, both the OMP carboxylate and Asp^{70} must be charged. The orotate carboxylate is certainly ionized at neutral pH in solution. Upon binding to the relatively hydrophobic environment of the enzyme's active site, however, the group's pK_a could shift and it could be protonated by water (*13*), especially since there is not sufficient space to accommodate solvating water molecules which could moderate electrostatic interactions. Alternatively, the lysines in the K^{42}D^{70}K^{72}D^{75B} chain could transfer protons to the neighboring aspartates, resulting in a neutral and relatively hydrophobic binding site for the substrate's aromatic ring. In our opinion, however, the results of the structural and stability studies performed on several mutants of *M. thermoautotrophicum* ODCase and discussed below are more consistent with charges residing on the alternating lysine and aspartate residues, with the enzyme showing an especially strong preference for a negative charge at the Asp^{70} position.

When Asp^{70} is mutated to an alanine and set up for crystallization in a solution containing OMP, UMP is found at the active site of the crystallized protein. Obviously, there is still enough catalytic power residing in this mutant enzyme to convert OMP to UMP over the rather long time frame of crystallization. At the same time, Lys^{42} and Lys^{72} sequestered a chloride ion from the medium to replace the aspartate's negative charge (Figure 2C), leading to a slight internal reorientation of the Lys^{72} side chain. Its C$_\beta$ atom moved 1.2 Å and the head ammonium group 1.6 Å. Surprisingly, this movement was not mirrored by Lys^{42}, the other amino acid flanking the mutation site; its position changed by less than 0.3 Å (Figure 2C).

When a larger void is created by mutating Asp^{70} to glycine and, at the same time, the more electronegative N6 of 6-azaUMP is placed close by, no chloride ion is found. Instead, several low-occupancy sites of water molecules lie between the side chains of Lys^{42} and Lys^{72}, the former showing only slightly increased movement whereas the latter adopts at least two alternate conformations. The disordered density of these two lysine residues is shown in Figure 2D. In addition, one again observes an even distribution between the syn- and anti-conformations of the nucleotide inhibitor (Figure 2D).

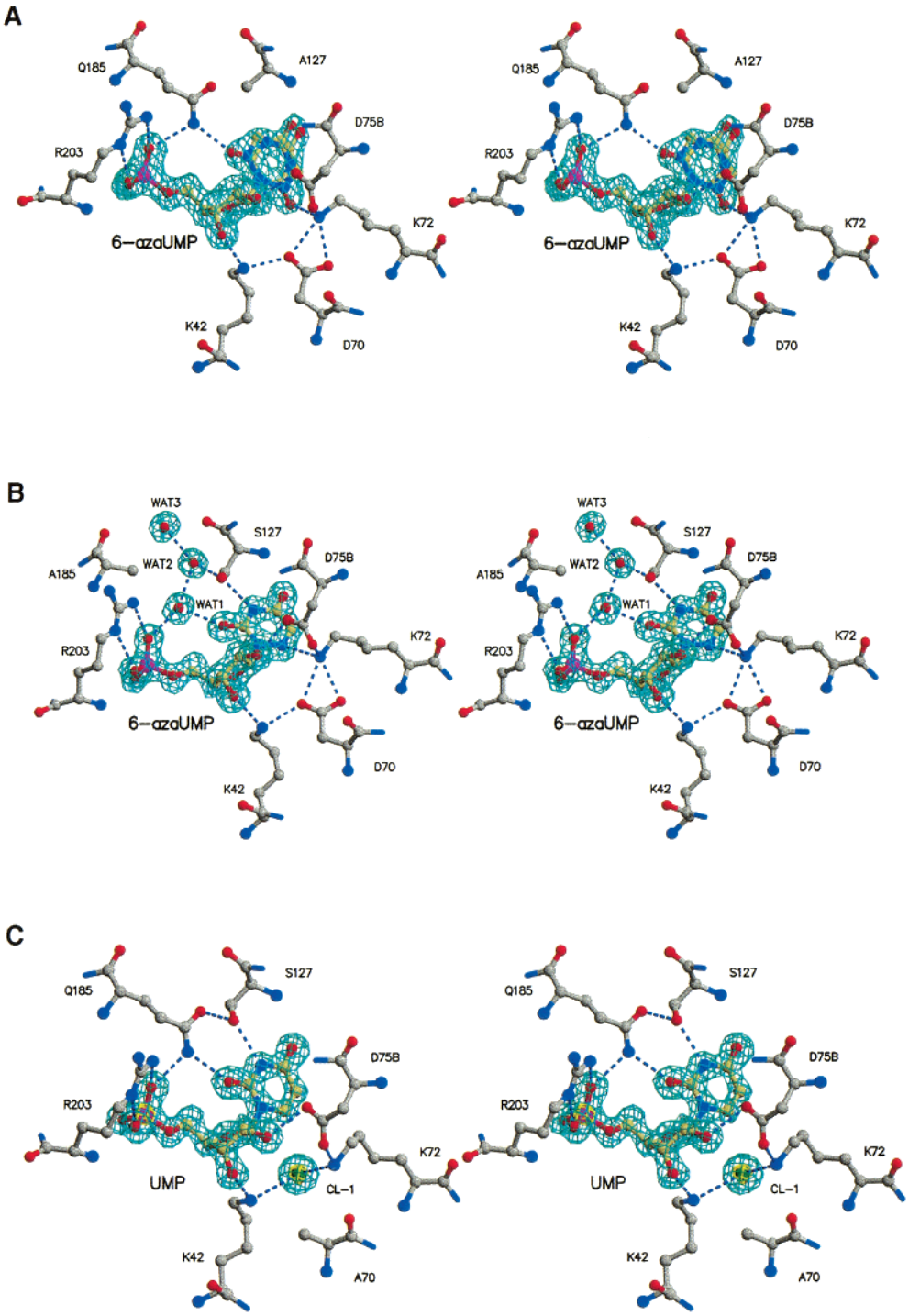

In the case of the D70N mutation, only the negative charge of the side chain is removed without changing its shape and space requirements; all azauracil rings are rotated around the N1−C4′ axis into an anti-conformation (Figure 2E). In the 6-azaUMP complexes of mutants which are unable to provide a negative charge at the position of the Asp^{70} carboxylate, a complete or partial base flip places an electron-rich oxygen atom in a position to counteract the charges of the two closely spaced lysines. This is mimicking the complex with the tightly binding competitive inhibitor 6-hydroxyuridine 5′-monophosphate (BMP) and seems to be preferred over the binding of an extraneous anion, which would have to be placed close to the electronegative N6 atom.

When $Asp75^{B}$, an active site residue contributed by the other monomer in the active dimer, is changed into an asparagine and the mutant protein complexed with 6-aza-UMP, the neutral asparagine swings out of the active site, in the largest movement of any side chain in any mutants seen so far. The place of the carboxylate group of Asp^{75B} is taken up by a spherical density that we interpreted as a Cl^{-} ion picked up from the crystallization buffer (Figure 2F). This ion also assumes the carboxylate's interactions with the ribose 2′-hydroxyl, Lys^{72}, and the backbone amide of Ile^{76}. The 6-azauracil ring sits right on top of this chloride ion, acting as the fourth ligand and completing a distorted tetrahedral coordination sphere. This type of aromatic ring−

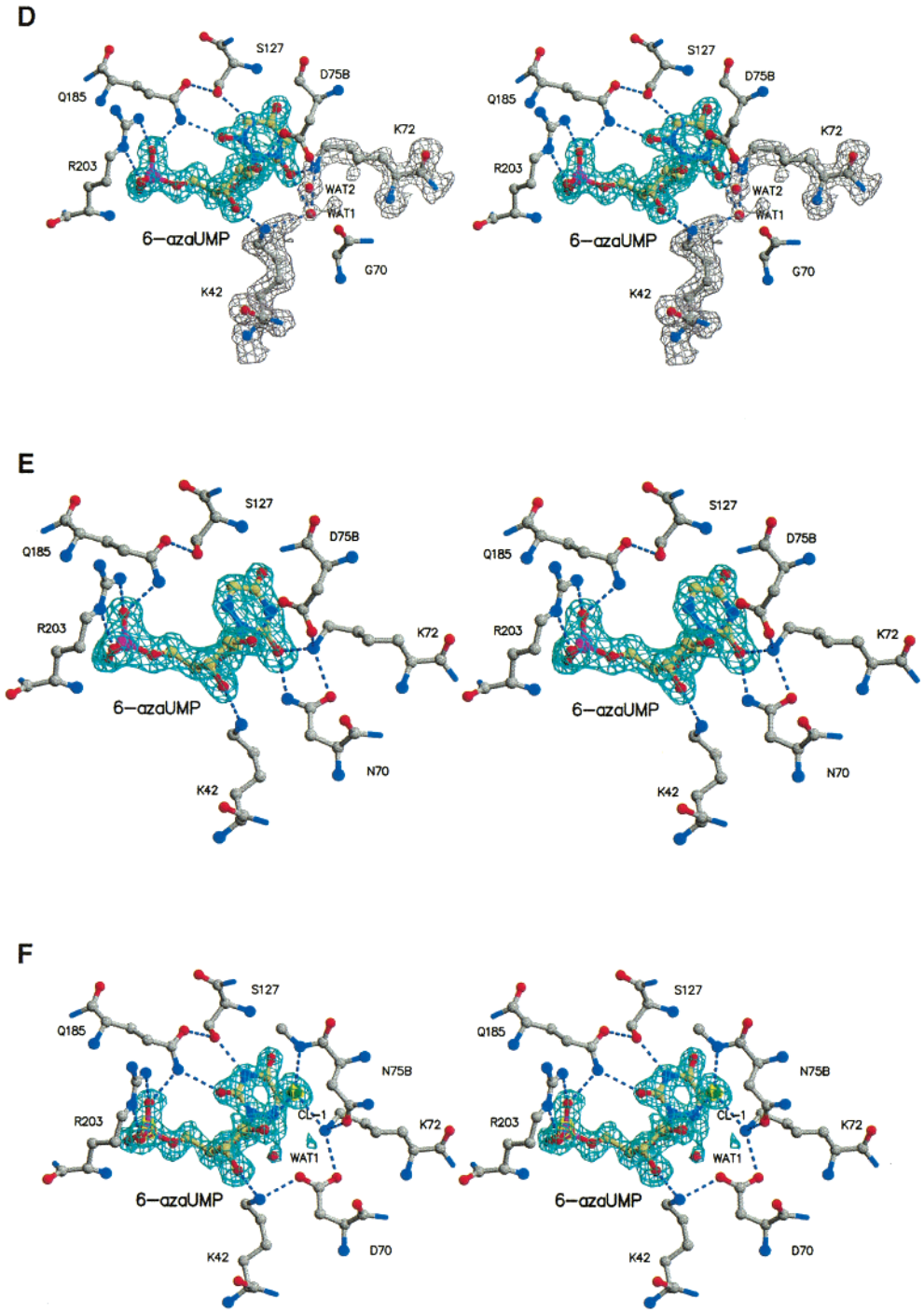

halogen ion interaction has been described before in small-molecule crystal structures (*29*).

Probing the Basic Residues of the Active Site's Alternating Charge Chain. To complement our mutational studies of the acidic residues contributing to the active site of ODCase, we also replaced both Lys^{42} and Lys^{72} by alanines. In the native structure, Lys^{42} undergoes two interactions: it forms a hydrogen bond to the 3′-hydroxyl of the ribose ring of OMP and presumably balances the negative charge of Asp^{70}. On the other hand, Lys^{72} bridges the two anionic residues Asp^{70} and Asp^{75B}, interacts with N6 of 6-azaUMP, and has been proposed to act as the proton donor to the carbanion, the intermediate formed in the catalyzed decarboxylation reaction (*30*). In both mutant structures, water molecules sit at the positions that were taken up by the ammonium groups of the respective lysine side chains (Figure 2G,H). Strong protein−substrate bonds have been replaced by less specific water-mediated interactions.

Effects of Various Mutations on Enzyme Stability. Removing the carboxylate side chains of the two aspartate residues in the active site results in the full or partial replacement of the lost negative charge close to the $K^{42}D^{70}K^{72}D^{75B}$ chain, either through recruitment of negatively charged ions from the crystallization medium or through reorientation of the ligand rings, placing atoms of higher electronegativity closer to the lysine side chains. In contrast to these findings, the removal of presumably positively charged lysine side chains resulted in the binding of water; in one case, the molecule was well-ordered whereas its position was less well-defined in the other case. However, no positive ions such as easily

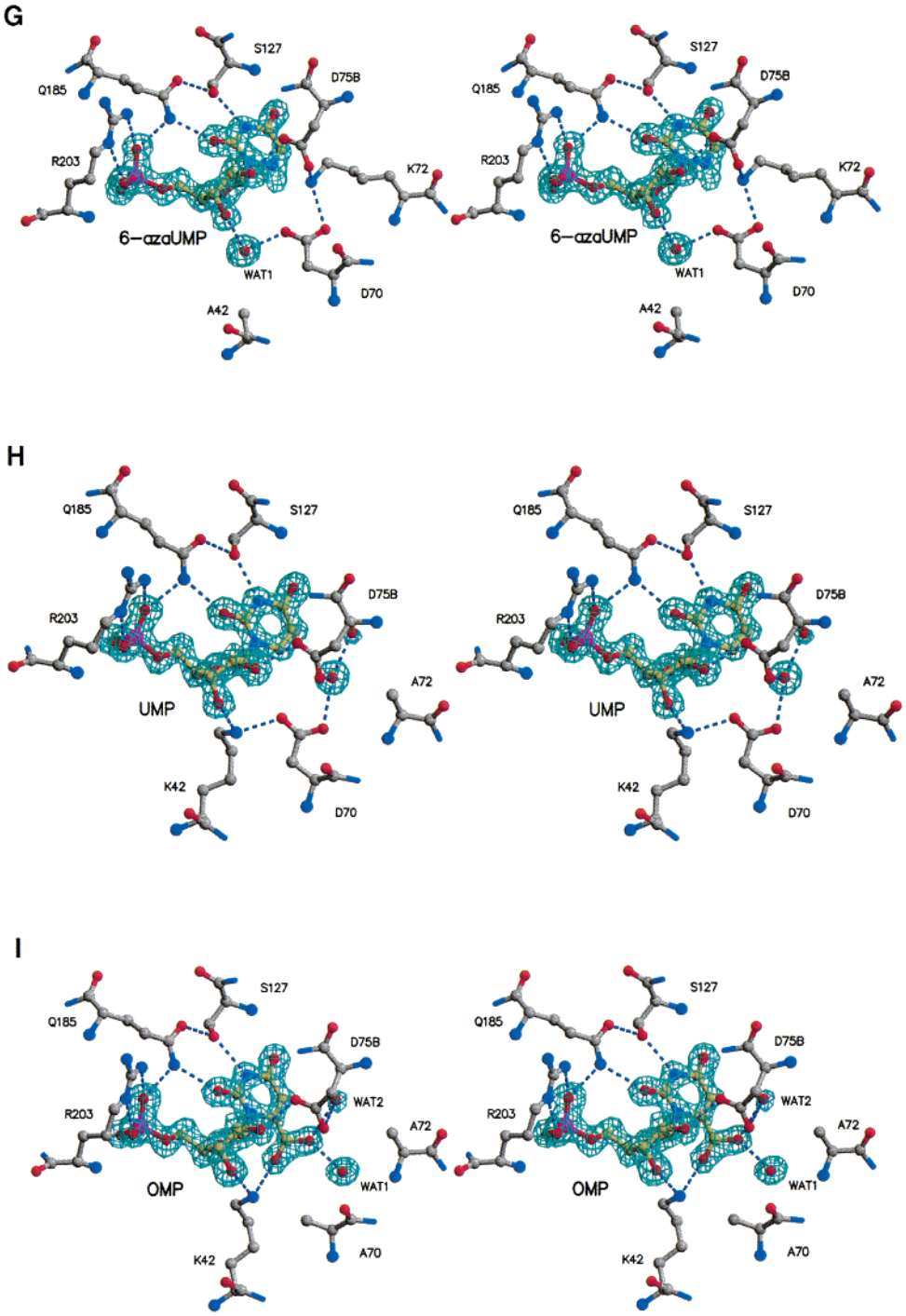

FIGURE 2: Stereoviews of mutant ODCase active sites. All densities are from $2F_o-F_c$ maps. (A) S127A/azaUMP, density contoured at 1.2σ and 1.6 Å resolution. (B) Q185A/azaUMP, density at 1.5σ, 1.5 Å. (C) D70A/UMP/Cl^-, blue density at 1.5σ, and yellow density at 8.5σ, 1.5 Å. (D) D70G/azaUMP, density at 1.1σ, 1.5 Å. (E) D70N/azaUMP, density at 1.8σ, 1.7 Å. (F) $D75^{B}N$/azaUMP, blue density at 1.4σ and yellow density at 8.5σ, 1.5 Å. (G) K42A/azaUMP, density at 1.2σ, 1.5 Å. (H) K72A/UMP, density at 1.5σ, 1.5 Å. (I) D70A/K72A/OMP, density at 1.4σ, 1.5 Å.

available sodium ions were taken up from the surrounding solution.

These structural results together with the observation that purification yields of various Asp^{70} mutants were drastically reduced when compared to native protein or the other mutants prompted us to investigate the role of this specific residue in protein stability. Unfortunately, high-temperature denaturation of *M. thermoautotrophicum* ODCase was not reversible (data not shown). GnHCl-induced unfolding studies, however, revealed interesting results (Figure 3). It was quite unexpected to see that the thermal stability of this protein (T_m > 70 °C) does not translate at all into chemical stability; the native protein unfolds in concentrations of less than 2 M GnHCl, reflecting clearly different mechanisms of unfolding for heat- and chemical-induced denaturation.

Both Asp^{70} mutants tested (D70G, D70A/K72A) were markedly less stable than native protein. In addition, the amount of GnHCl required to reach the transition point increased with increasing protein concentration. The K72A mutant shows a similar concentration dependence, but its

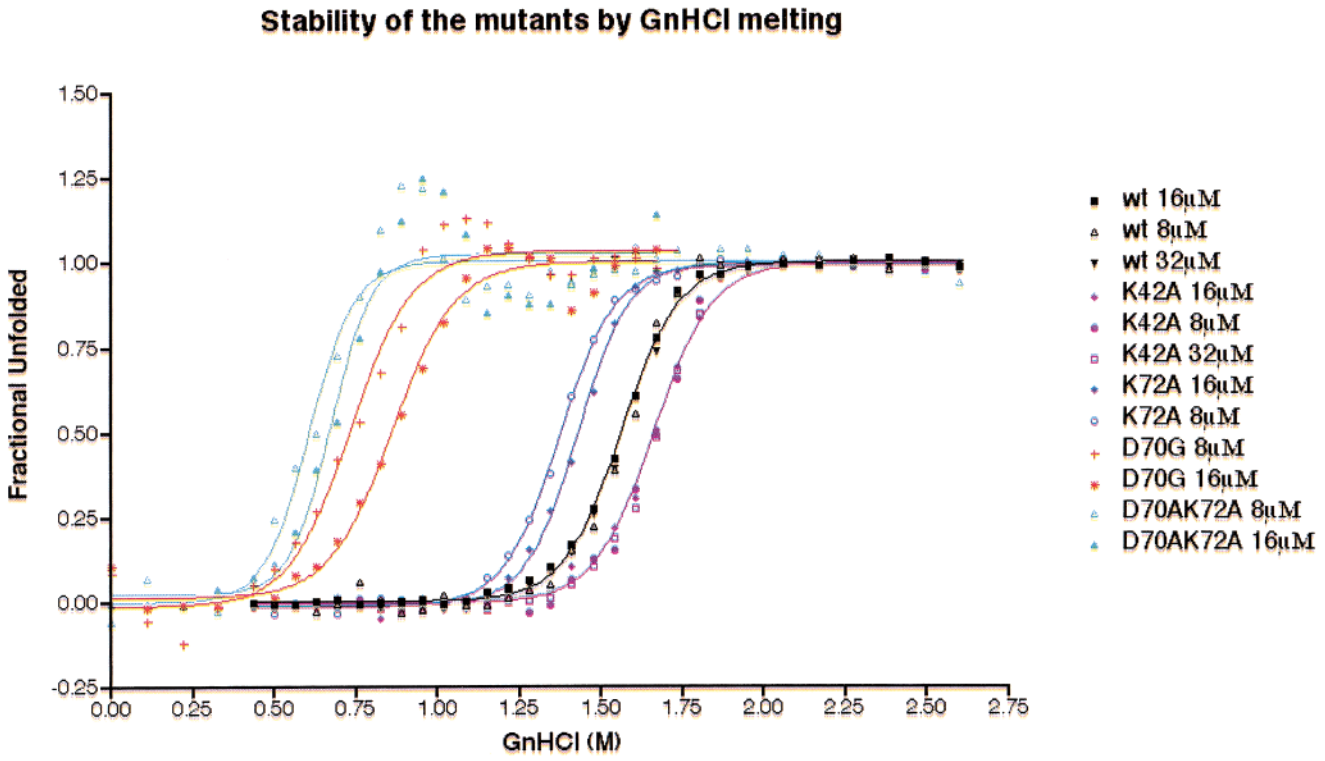

FIGURE 3: Guanidine hydrochloride denaturation of the native and mutant ODCase. Chemical denaturation was monitored by measuring the CD signal at 222 nm on samples with protein concentrations ranging from 8 to 32 μM at 25 °C. The lines joining the points are the theoretical fits to the data obtained using the program Prism (*26*). The denaturation curve is in black for native protein, in purple for the K42A mutant, in blue for the K72A mutant, in red for the D70G mutant, and in green for the D70AK72A double mutant.

stability is almost the same as that of the native protein. The K42A mutant, however, is slightly more stable than the native protein, and its melting curve is independent of protein concentration.

In the case of the K72A mutant, the dependence on protein concentration could be explained by an increase of the dimer dissociation constant upon loss of the residue's interaction with Asp^{75B} from the other monomer. Asp^{70}, however, is not involved in any contacts at the dimer interface. The reduced stability of D70G, in addition, seems to support the notion that the active site has evolved to require a negative charge at the position of the Asp^{70} side chain. Such an interpretation could also explain the small but significant increase in stability shown by the K42A mutant since the removal of a positive charge so close to the position of Asp^{70} should reinforce the negative potential of this site.

Obviously, it would be beneficial to have the melting curves of all aspartate mutants. However, the purification yields for D70A and D70N were very low, making meaningful measurements extremely difficult. To make things worse, all these mutants showed a tendency to precipitate in the course of hours (see legend to Figure 3), a process that interfered with proper equilibration. The Asp^{75B} mutant was the most precipitation-prone one but provided quite satisfactory yields during purification. Clearly, the absence of negative charges at the carboxylate positions of Asp^{70} and Asp^{75B} drastically reduces not only the catalytic efficiency of ODCase (*16*) but also its stability. In our opinion, this would argue that the most proficient enzyme known has evolved to maintain a series of alternating charges at its catalytic site, which in turn would be consistent with charge−charge repulsion contributing in a significant way to the catalytic mechanism.

Residual Catalytic Activity in Active Site Mutants. As previous studies on yeast ODCase (*16*) had shown that changing the aspartate residue corresponding to Asp^{70} resulted in essentially inactive enzyme, we set up the D70A mutant protein for crystallization in a solution containing OMP and quickly obtained crystals. However, the electron density map calculated from the diffraction pattern collected from these crystals clearly revealed that instead of substrate a molecule of the product UMP was bound at the active site. Next to it, between the side chains of Lys^{42} and Lys^{72}, there was a spherical peak whose shape, height, and coordination pattern were consistent with those of a chloride ion, most probably sequestered from the crystallization buffer. It is conceivable that such an ion, taking the place of the aspartate carboxylate, could also be used to exert electrostatic stress on the orotidine carboxylate as well as keep the neighboring lysine side chains locked in place. Obviously, the D70A mutant retained sufficient catalytic power to transform OMP to UMP given the high protein concentrations and extended periods of time needed for crystal formation. The mutant's low but measurable catalytic activity was established in an optical assay monitoring absorbance at 285 nm at room temperature (data not shown). In an effort to prevent catalytic turnover, we tried extensive dialysis to eliminate any small anions (such as Cl^-) from the protein solution used for crystallization, but once again the electron density was only consistent with an UMP ligand accompanied by diffuse density at the former chloride binding site (data not shown).

Kinetic studies have identified Lys^{72} as the residue that protonates the C6 carbanion; its removal led to a catalytically incompetent enzyme (*30*). Similar to what has been described above, however, OMP added to crystallization solutions was converted to UMP as identified from the electron density

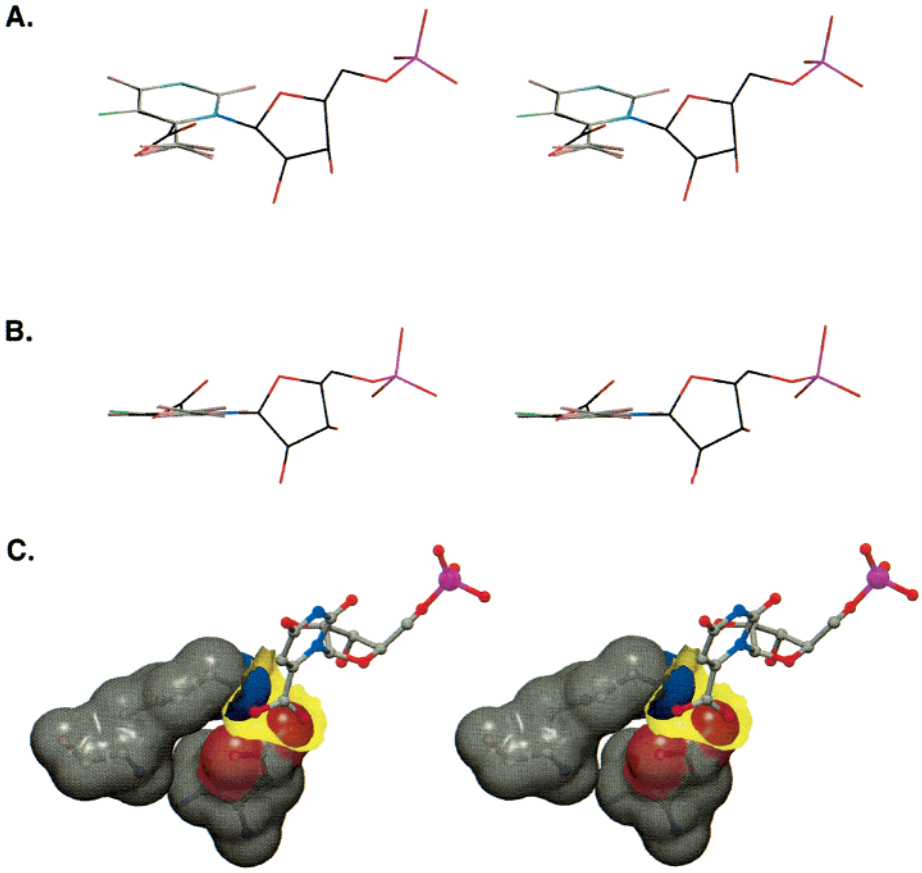

FIGURE 4: (A and B) Stereoview of OMP (dark colors) as bound to the D70A/K72A double mutant active site compared to the seven orotate crystal structures found in the Cambridge Structural Database (light colors; *32*). (C) Interpenetration of the van der Waals surfaces of orotate's C6 carboxylate (yellow) and Asp70 (red) as well as Lys72 (blue) in the active site of native *M. thermoautotrophicum* ODCase.

maps of the complex. In this case, the proton needed for neutralizing the carbanion intermediate may come from a water molecule, which takes up the position of the Lys^{72} amino group. As with the Asp^{70} mutants, it seems that the long time spans and high enzyme concentrations of crystallization experiments revealed very low residual catalytic activity unobserved in kinetic experiments.

A Substrate with a Twist. Only with both Asp^{70} and Lys^{72} mutated to alanines were we able to observe the substrate OMP bound at the active site (Figure 2I). Simultaneous removal of these two residues obviously reduced the catalytic potential of ODCase sufficiently to prevent the conversion of substrate to product. Several examples of orotate structures are found in the Cambridge Structural Database (*31*). They all (CSD codes: AMOROT, RBFORM, SIM2UJ, CEXBEM10, OROTAC, YAVHOS, FASBEG) show the carboxylate group in plane with the aromatic ring. In contrast, OMP, when bound to the ODCase double mutant D70A/K72A, assumed a higher energy conformation. Its carboxylate group was rotated 30° out of the plane, and the C6−C7 bond was no longer coplanar with the pyrimidine ring, placing C7 0.3 Å and one of the oxygen atoms 1.1 Å off the plane, respectively (Figure 4). This oxygen atom tilted into the cavity which had been suggested as a transient binding site for the product CO_2 (*10*). In the catalytically inactive double mutant, the two alanine side chains provided space not found in the native enzyme. In this void, the D70A/K72A mutant bound two water molecules, one of which was very well-ordered and bridged the OMP carboxylate with the Ala^{72} amide. These water molecules partially shield the negative charge of the carboxylate. If the structure of orotate is distorted toward a higher energy conformation under such mitigating circumstances, one can safely assume that much stronger forces will act on it in the native enzyme. For one, modeling OMP into the active site of native enzyme creates serious steric clashes between the carboxylate group and the side chains of both Asp^{70} and Lys^{72}, on top of any charge−charge interactions. One of the carboxylate oxygens would be only 1.8 Å away from the side chain nitrogen of Lys^{72}, and the other oxygen atom would sit at the same distance from Asp^{70} (Figure 4).

CONCLUSIONS

Given the transformation of OMP to UMP in the D70A mutant, the negative charge on Asp^{70} cannot be the only driving force for decarboxylation. The same argument can be made for Lys^{72} and its potential to protonate the intermediate carbanion at C6. Steric hindrance created by the side chains of these two residues would prevent binding of undistorted substrate. Major readjustments of the active site itself do not seem to be easily accessible given the very small degree of structural variability (rmsd less than 0.6 Å for 45 atoms in the active site) seen in the many analyses of ODCases from four sources with three different inhibitors, product, and now substrate (*10*−*13*), all crystallized from different pH's and precipitant conditions, with different crystal packing. This stable arrangement argues strongly that main and side chain atoms assume orientations of relatively

low overall energy. This would also be in line with the results of recent isothermal titration calorimetry experiments (*16*) that could not detect any binding of OMP to D91A and K93A mutants of the yeast enzyme (corresponding to D70A and K72A, respectively, in *M. thermoautotrophicum*). The removal of one of the side chains at a time does not seem to produce a mutant enzyme capable of binding OMP with a measurable affinity.

We envision progress of ODCase catalysis as a series of 'binding' and 'forcing' events. As OMP approaches the enzyme's active site, the 5′-phosphate group serves as a first anchoring point with high binding energy. Then, the clamping down of four bonds to the hydroxyl groups of ribose not only draws the remaining parts of the substrate molecule into the active site, but also brings the two monomers closer together, forming a tighter active site. The driving force created by the binding of the phosphoribose group is absolutely necessary for correct placement of the orotate ring. Without it, the base does not bind, as was nicely shown with radioactively labeled orotic acid (*19*). Decarboxylation is initiated while the orotate ring is brought close to the negative charge of Asp^{70}, and, at the same time, it experiences the steric resistance exerted by a binding site too small for a comfortable fit of the intact orotate ring. CO_2 released might transiently bind in an adjacent and properly sized cavity (*10*), creating the C6 carbanion intermediate. It is during this process that all enzyme−ligand interactions are achieved and the binding energy is maximized (*16*). The preferred binding of molecules such as 6-azaUMP and BMP would reflect their similarity to the transition state rather than to the substrate.

Lys^{72} protonates the C6 carbon, leaving it uncharged. The unbalanced charges of the adjacent aspartates lead to a loosening of the dimer interactions, allowing product release. Transfer of a proton from bulk solvent to Lys^{72} closes the catalytic cycle.

Evolution has selected an intricate arrangement of backbone and side chain atoms that creates a finely tuned potential at the active site of ODCase, balancing their contributions to the stability of the enzyme's fold and their potential contributions to catalysis as shown for Asp^{70}. It does not seem unreasonable to assume that an enzyme, which has developed into the most proficient protein catalyst we know, accelerating the decarboxylation of a very stable substrate by 17 orders of magnitude without the help of metal ions, cofactors, or delocalization effects, has to make use of any and all effects available.

ACKNOWLEDGMENT

We thank the staff at BioCARS for their dedicated help and support.

REFERENCES

1. Radzicka, A., and Wolfenden, R. (1995) *Science 267*, 90−93.
2. O'Leary, M. H. (1992) *Enzymes (3rd Ed.) 20*, 235−269.
3. Miller, B. G., Smiley, J. A., Short, S. A., and Wolfenden, R. (1999) *J. Biol. Chem. 274*, 23841−23843.
4. Cui, W., DeWitt, J. G., Miller, S. M., and Wu, W. (1999) *Biochem. Biophys. Res. Commun. 259*, 133−135.
5. Beak, P., and Siegel, B. (1976) *J. Am. Chem. Soc. 98*, 3601−3606.
6. Acheson, S. A., Bell, J. B., Jones, M. E., and Wolfenden, R. (1990) *Biochemistry 29*, 3198−3202.
7. Lee, J. K., and Houk, K. N. (1997) *Science 276*, 942−945.
8. Rishavy, M. A., and Cleland, W. W. (2000) *Biochemistry 39*, 4569−4574.
9. Rouhi, A. M. (2000) *C&EN Washington March 13*, 42−46.
10. Wu, N., Mo, Y., Gao, J., and Pai, E. F. (2000) *Proc. Natl. Acad. Sci. U.S.A. 97*, 2017−2022.
11. Miller, B. G., Hassell, A. M., Wolfenden, R., Milburn, M. V., and Short, S. A. (2000) *Proc. Natl. Acad. Sci. U.S.A. 97*, 2011−2016.
12. Appleby, T. C., Kinsland, C., Begley, T. P., and Ealick, S. E. (2000) *Proc. Natl. Acad. Sci. U.S.A. 97*, 2005−2010.
13. Harris, P., Navarro Poulsen, J. C., Jensen, K. F., and Larsen, S. (2000) *Biochemistry 39*, 4217−4224.
14. Houk, K. N., Lee, J. K., Tantillo, D. J., Bahmanyar, S., and Hietbrink, B. N. (2001) *Chembiochem. 2*, 113−118.
15. Warshel, A., Florián, J., Štrajbl, M., and Villà, J. (2001) *Chembiochem. 2*, 109−111.
16. Miller, B. G., Snider, M. J., Wolfenden, R., and Short, S. A. (2001) *J. Biol. Chem. 276*, 15174−15176.
17. Miller, B. G., Butterfoss, G. L., Short, S. A., and Wolfenden, R. (2001) *Biochemistry 40*, 6227−6232.
18. Jencks, W. P. (1975) *Adv. Enzymol. Relat. Areas Mol. Biol. 43*, 219−410.
19. Miller, B. G., Snider, M. J., Short, S. A., and Wolfenden, R. (2000) *Biochemistry 39*, 8113−8118.
20. Wu, N., Christendat, D., Dharamsi, A., and Pai, E. F. (2000) *Acta Crystallogr., Sect. D: Biol. Crystallogr. 56*, 912−914.
21. Wright, D. A., Park, S. K., Wu, D., Phillips, G. J., Rodermel, S. R., and Voytas, D. F. (1997) *Nucleic Acids Res. 25*, 2679−2680.
22. Otwinowski, Z., and Minor, W. (1997) *Methods Enzymol. 276*, 307−326.
23. Brunger, A. T., Adams, P. D., Clore, G. M., DeLano, W. L., Gros, P., Grosse-Kunstleve, R. W., Jiang, J. S., Kuszewski, J., Nilges, M., Pannu, N. S., Read, R. J., Rice, L. M., Simonson, T., and Warren, G. L. (1998) *Acta Crystallogr., Sect. D: Biol. Crystallogr. 54*, 905−921.
24. Kissinger, C. R., Gehlhaar, D. K., and Fogel, D. B. (1999) *Acta Crystallogr., Sect. D: Biol. Crystallogr. 55*, 484−491.
25. Jones, T. A., Zou, J. Y., Cowan, S. W., and Kjeldgaard (1991) *Acta Crystallogr. A47*, 110−119.
26. Prism, GraphPad Software Inc., http://www.graphpad.com.
27. Saenger, W. (1973) *Angew. Chem., Int. Ed. Engl. 12*, 591−601.
28. Traut, T. W., and Temple, B. R. (2000) *J. Biol. Chem. 275*, 28675−28681.
29. Momotake, A., Mito, J., Yamaguchi, K., Togo, H., and Yokoyama, M. (1998) *J. Org. Chem. 63*, 7207−7212.
30. Smiley, J. A., and Jones, M. E. (1992) *Biochemistry 31*, 12162−12168.
31. Cambridge Structural Database (CSD), http://www.ccdc.cam.ac.uk/prods/csd/csd.html.

BI015758P